



## Atomic Layer Deposition of Ru Thin Films Using 2,4-(Dimethylpentadienyl)(ethylcyclopentadienyl)Ru by a Liquid Injection System

Seong Keun Kim,<sup>a</sup> Sang Young Lee,<sup>a</sup> Sang Woon Lee,<sup>a</sup> Gyu Weon Hwang,<sup>a</sup>  
Cheol Seong Hwang,<sup>a,z,\*</sup> Jin Wook Lee,<sup>b</sup> and Jaehack Jeong<sup>b</sup>

<sup>a</sup>School of Materials Science and Engineering and Interuniversity Semiconductor Research Center, Seoul National University, Seoul 151-744, Korea

<sup>b</sup>Quros Company, Sunnam, Kyunggi-do 462-120, Korea

Ru thin films were grown on Si, SiO<sub>2</sub>, TiO<sub>2</sub>, and TiN substrates by atomic-layer deposition using 2,4-(dimethylpentadienyl)(ethylcyclopentadienyl)Ru and O<sub>2</sub> as Ru precursor and reactant, respectively, at temperatures ranging from 230 to 280°C. A saturated growth rate of 0.04 nm/cycle and a low oxygen concentration (below the detection limit of Auger electron spectroscopy) were obtained at 250°C. The Ru film showed a negligible incubation period on all the different types of substrates, and an active nucleation behavior which resulted in a very smooth film surface morphology. The dimethylpentadienyl ligand enhanced the active nucleation of Ru and retarded the oxidation of the grown Ru layer. Good step coverage (>90%) was obtained from the Ru film grown on a capacitor hole with an aspect ratio of 17 and an opening diameter of 150 nm by a proper control of the Ar carrier gas flow rate.

© 2007 The Electrochemical Society. [DOI: 10.1149/1.2403081] All rights reserved.

Manuscript submitted July 3, 2006; revised manuscript received September 25, 2006. Available electronically January 4, 2007.

The deposition of Ru thin films either by metallorganic chemical vapor deposition (MOCVD) or atomic-layer deposition (ALD) has been extensively studied in recent years using various types of precursors including carbonyl,  $\beta$ -diketonates, and cyclopentadienyl compounds of Ru for its application in capacitors of dynamic random access memory (DRAM) or as diffusion barrier in Cu-metallization.<sup>1-10</sup> For both applications, the conformal deposition over severe three-dimensional structures with thin and uniform microstructures is the essential factor. MOCVD and ALD have been considered as the proper process for Ru thin-film deposition for these applications. As DRAM devices scale down, a better step coverage over severe three-dimensional contact hole structure (aspect ratio >15) and smaller thickness of the Ru film (<10 nm) are required. Although MOCVD appears to have several merits such as higher growth rate, ALD becomes crucial for satisfying these requirements. ALD has the merits of a better step coverage and thickness controllability, although it has its own demerits such as a lower growth rate. However, as the necessary thickness of the Ru film becomes smaller, <10 nm, and faster processing technology, such as semibatch type deposition systems, is developed, ALD appears to be more proper for the Ru film deposition process.

MOCVD and ALD of Ru films are preceded by oxidative decomposition of  $\beta$ -diketonate, such as Ru(C<sub>11</sub>H<sub>19</sub>O<sub>2</sub>)<sub>3</sub> [Ru(thd)<sub>3</sub>],<sup>4,5</sup> and cyclopentadienyl Ru precursors, such as Ru(C<sub>5</sub>H<sub>5</sub>)<sub>2</sub> [Ru(Cp)<sub>2</sub>] (Ref. 6 and 10) and Ru(C<sub>2</sub>H<sub>5</sub>C<sub>5</sub>H<sub>4</sub>)<sub>2</sub> [Ru(EtCp)<sub>2</sub>].<sup>11-13</sup> Although carbonyl-based precursors, such as Ru<sub>3</sub>(CO)<sub>12</sub>,<sup>2,3</sup> are used to grow Ru films without the help of oxidant, the resulting films are usually impure, which makes them less suitable. Oxygen plays a key role in the Ru film deposition in both MOCVD and ALD using  $\beta$ -diketonate and cyclopentadienyl as Ru precursors. The removal of the ligands is certainly improved by the addition of oxygen, whereas the oxidation of deposited Ru is limited to a low degree by kinetic reasons.<sup>5,11</sup> Most of the supplied oxygen is consumed by oxidation of C and H derived from the ligand because they have a higher oxidation potential than Ru.<sup>5,11</sup> When the precursor is delivered as a solution form in the liquid delivery technique, as in this experiment, the oxygen consumption by the solvent is even more serious. The residual oxygen in Ru films induces several serious problems in the integrated devices, especially during high temperature (>600°C) postdeposition processes: oxidation of underlying barrier layers and deterioration of the structural stability in DRAM capacitors.<sup>14</sup> Kwon

et al. used NH<sub>3</sub> plasma instead of oxygen as reactant in their plasma-enhanced ALD (PEALD) process of Ru film to avoid this problem. They showed that Ru films with a very low impurity concentration and a reasonable saturated growth rate (0.038 nm/cycle) can be obtained.<sup>15</sup> However, the PEALD required a complex hardware for the plasma power application, and step coverage was not reported.

In thermal MOCVD or ALD (without plasma) the impurity concentration is dependent on the precursors. The research group at Helsinki University reported that the Ru ALD using Ru(thd)<sub>3</sub> and Ru(Cp)<sub>2</sub> and air as reactant showed a rather different growth behavior and residual impurities even with the same reactors and under almost identical deposition conditions.<sup>4,6</sup> The saturated ALD growth rate ( $G_r^{\text{sat}}$ ) was almost identical (~0.04 nm/cycle). They also reported very comprehensive works on the ALD mechanism for Ru films using a quadruple mass spectrometer and quartz crystal microbalance.<sup>4,10</sup> It was concluded that oxygen was adsorbed on the grown Ru surface which reacted with the incoming Ru precursors during the subsequent Ru pulse step. The reaction reduced the Ru(O) film by liberating H<sub>2</sub>O and CO<sub>2</sub>. During the oxygen pulse step the remaining ligands of the adsorbed Ru precursor reacted with oxygen producing H<sub>2</sub>O and CO<sub>2</sub> as reaction by-products as well. It was clearly shown that oxygen existed at the subsurfaces of the Ru film during ALD, although it was mostly removed during the subsequent steps.<sup>10</sup> However, it is also probable that the removal of the oxygen is not complete depending on the process conditions (short reaction cycle) and precursors (less reactive precursor).

Another concern about the Ru MOCVD or ALD is the difficult nucleation of the film on SiO<sub>2</sub> and TiN, which are the two contacting surfaces of Ru layers in integrated structures. This was observed both in ALD using Ru(Cp)<sub>2</sub> (Ref. 6) and Ru(thd)<sub>3</sub> (Ref. 4) and MOCVD using Ru(EtCp)<sub>2</sub>,<sup>12,16</sup> where the retardation of film growth was observed during the initial period of the deposition process. This might be understood from the growth mechanism of a Ru film suggested by the Helsinki group.<sup>4,10</sup> The oxidative adsorption and decomposition of Ru precursor on a predeposited Ru layer is largely facilitated by the reaction between the ligands of incoming Ru precursor and adsorbed oxygen on the predeposited Ru layer. If the oxygen adsorption on the substrate surface is not active, or the donation of the preadsorbed oxygen to the ligands of coming Ru precursor is limited by the strong bonding between the surface and oxygen, the Ru nucleation might be suppressed. Once Ru nuclei are formed the Ru growth mechanism is actively working on the Ru nuclei and a steady Ru growth rate is achieved. Therefore, it can be

\* Electrochemical Society Active Member.

<sup>z</sup> E-mail: cheolsh@snu.ac.kr

anticipated that the initial growth of Ru on a  $\text{SiO}_2$  and TiN surface is dependent on the chemical adsorption or thermal decomposition property of the Ru precursors. Especially in ALD, where the thermal decomposition or oxidative decomposition of the Ru precursor is suppressed, the active adsorption property of the precursor on such a less-active (in terms of the oxygen activity) surface is the crucial factor for obtaining active nucleation and uniform film growth.

It can be anticipated that the chemisorption of  $\text{Ru}(\text{Cp})_2$  and  $\text{Ru}(\text{EtCp})_2$  on these substrates is not easy considering the stable bonding nature between Ru and Cp ligands due to the  $\pi$ -conjugation of valence electrons in the Cp rings. The preadsorbed oxygen is necessary to induce the oxidative dissociation of these Cp rings, as mentioned previously, but the  $\text{SiO}_2$  and TiN surfaces are not favorable for the adsorption and subsequent supply of oxygen to the incoming  $\text{Ru}(\text{Cp})_2$  or  $\text{Ru}(\text{EtCp})_2$ .

Recently, Shibutani et al. used 2,4-(dimethylpentadienyl) (ethylcyclopentadienyl)Ru (DER) as Ru precursor with the help of oxygen in the MOCVD process.<sup>16</sup> They reported that the MOCVD with DER involves negligible initial growth retardation compared to the  $\text{Ru}(\text{EtCp})_2$  case. It is believed that the dimethylpentadienyl (DMPD) ligand of the DER facilitates the initial adsorption of the Ru precursor onto the  $\text{SiO}_2$  and TiN surface which enhances the subsequent Ru film growth. They compared the thermal decomposition behavior of the two precursors [DER and  $\text{Ru}(\text{EtCp})_2$ ] using differential scanning calorimetry under a  $\text{N}_2$  atmosphere, and found that the DER is more vulnerable to thermal decomposition compared to  $\text{Ru}(\text{EtCp})_2$  (thermal decomposition temperature was lower by  $\sim 100^\circ\text{C}$ ). This might be due to the less stable bonding between the DMPD ligand and Ru ions. It is also probable that once the DMPD ligand dissociates from the precursor molecule, the bonding between the remaining EtCp ligand and Ru ions also becomes less stable and finally the thermal decomposition occurs at a lower temperature. Therefore, it is reasonable to assume that the DER precursor also results in a better deposition property by ALD by reducing the incubation period.

In this paper, the ALD behavior of Ru films using DER precursor is reported in detail. The step coverage of the Ru film on a severe three-dimensional structure (hole structure with a diameter of 150 nm and an aspect ratio of 17) is investigated considering the next-generation DRAM application.

### Experimental

Ru films were deposited using an 8 in. diameter wafer scale (shower head diameter of 12 in.) shower-head type ALD reactor (Quoros, Co., Plus-200) at growth temperatures ranging from 230 to  $280^\circ\text{C}$ . The ALD system was equipped with a liquid injection system for feeding Ru precursor into the reactor. DER (Tosoh, Co.) precursor dissolved in ethylcyclohexane (ECH) with a concentration of 0.2 M was used as Ru source. The molecular structure of DER is shown in Fig. 1.  $\text{O}_2$  was used as reactant and the  $\text{O}_2$  gas flow rate was varied from 300 to 1000 sccm. Ar gas with a flow rate ranging from 30 to 500 sccm was used as carrier gas, and Ar gas with a flow rate of 1000 sccm was used as purge gas. ALD  $\text{TiO}_2$ , sputtered TiN, thermal  $\text{SiO}_2$  films on Si wafers and bare Si(100) wafers were used as substrates in order to investigate substrate-dependent deposition properties of metallic Ru films. Also, Ru films were deposited on a capacitor hole structure formed in  $\text{SiO}_2$  substrates with an aspect ratio  $\sim 17$  to investigate the step coverage of Ru films.

A deposition cycle for Ru films consisted of four steps: Ru source feeding-purge-oxygen feeding-purge. Because a liquid delivery method was adopted for the Ru solution source, the precursor solution was pressurized by Ar gas and was fed into the hot vaporizer (maintained at  $200^\circ\text{C}$ ) through an electrically controlled nozzle. The amount of precursor solution supply was controlled by changing the opening time of the nozzle from 6 to 15 ms. The precursor solution was flash evaporated in the vaporizer and carried into the reactor with the help of Ar carrier gas, the flow rate of which was

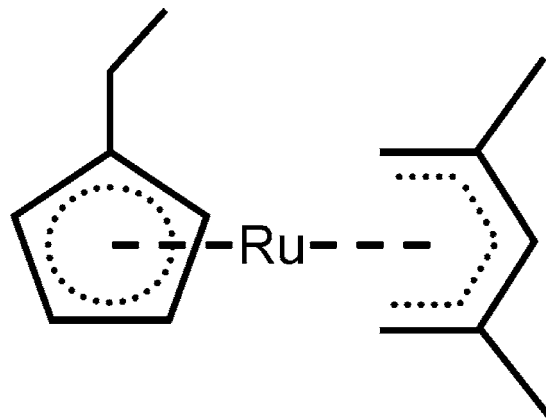


Figure 1. The molecular structure of DER precursor.

changed from 30 to 500 sccm. The Ar carrier injection time was also changed from 1 to 5 s. The total amount of precursor that was supplied to the reactor during the Ru source feeding step was controlled either by the solution injection time or Ar carrier gas injection time. Typical purge time after the Ru source feeding and  $\text{O}_2$  pulse steps was 5–8 s, which was long enough to confirm that the film growth rate was saturated with this purge time.

The film thickness was measured by field-emission scanning electron microscopy (FESEM) and cross-sectional high-resolution transmission electron microscopy (HRTEM). Due to the relatively small thickness of the Ru films deposited in this experiment (15–35 nm), thickness measurement by FESEM had a limited accuracy. Therefore, the area density of Ru films measured by X-ray fluorescence spectroscopy (XRF) was used to check the saturation behavior of the film growth. The sheet resistance of Ru thin films was measured by a four-point probe at room temperature. The crystalline structure of the Ru thin films was investigated by X-ray diffraction (XRD) using  $\text{Cu K}\alpha$  radiation. The impurity concentration, including oxygen, in the films was investigated by Auger electron spectroscopy (AES).

### Results and discussion

Figure 2a and b shows the variations in the area density of a Ru film deposited on a Si substrate as a function of the Ru source injection time and Ar carrier gas injection time, respectively, at a growth temperature ( $T_g$ ) of  $250^\circ\text{C}$ . Here, the  $\text{O}_2$  flow rate and pulse time were 1000 sccm and 3 s, respectively, and the number of deposition cycles ( $n_{\text{cy}}$ ) was 300. In a and b, the Ar carrier gas injection time and Ru source injection time were 3 s and 6 ms, respectively. The area density was independent of the source and carrier gas input time, suggesting that the ALD process worked under these conditions. Although the Ar carrier gas injection time had a negligible

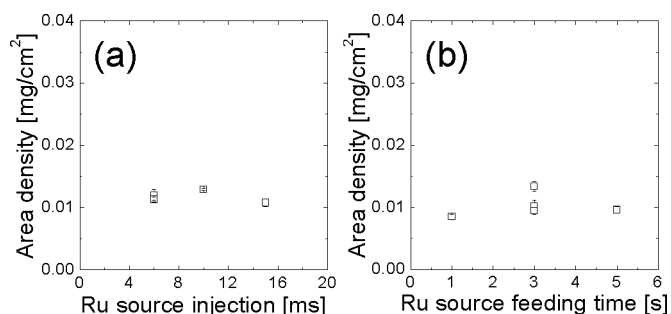
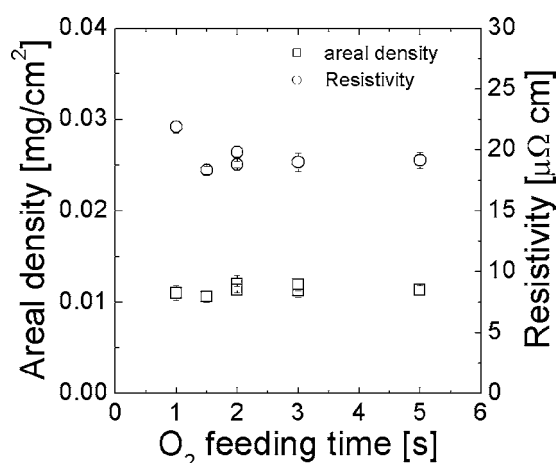


Figure 2. The variations in the area density of a Ru film grown on a Si substrate as a function of (a) the Ru source injection time, (b) Ar carrier gas injection time.



**Figure 3.** The variations in the area density and resistivity of a Ru film grown on a Si substrate as a function of the  $O_2$  gas injection time.

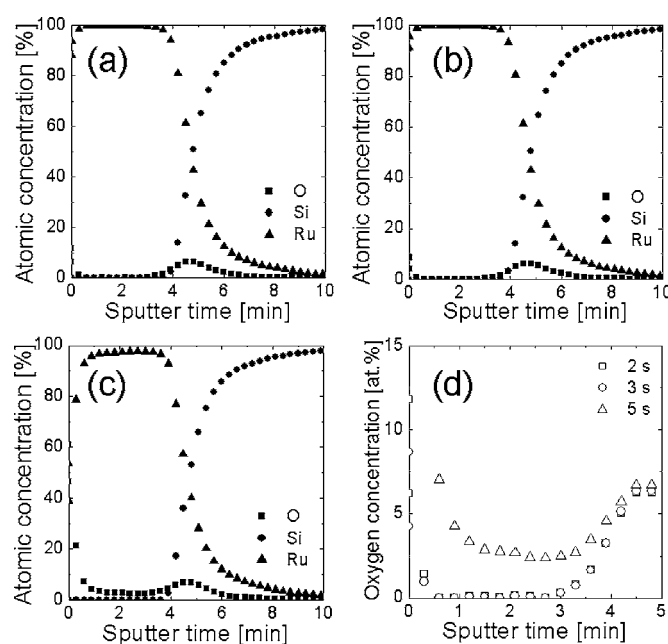
influence on the growth rate ( $G_r$ ) of the Ru films on Si substrates, the flow rate of the Ar carrier gas had a profound effect on the step coverage on the hole structure, as shown later.

Figure 3 shows the variations in the area density of a Ru film deposited on a Si substrate as a function of the  $O_2$  gas injection time, where the  $O_2$  flow rate, Ru source injection time, and Ru carrier gas injection time were 1000 sccm, 6 ms, and 3 s, respectively. The area density was almost independent of the  $O_2$  gas injection time, ranging from 1 to 5 s, suggesting that the saturated growth behavior of the ALD Ru process was also confirmed with respect to the  $O_2$  flow rate. The variation of the resistivity of the film calculated from the sheet resistance and film thickness is also shown in Fig. 3. The resistivity was saturated to  $\sim 19 \mu\Omega \text{ cm}$  with increasing  $O_2$  injection time. These values are rather high compared to the bulk value of Ru ( $7.2 \mu\Omega \text{ cm}$ ). However, this is comparable to other reports on Ru thin films grown by MOCVD or ALD.<sup>6,8,17</sup> Considering the small thickness of the Ru films grown here ( $\sim 10 \text{ nm}$ ), a resistivity of  $19 \mu\Omega \text{ cm}$  is a reasonable value. The density of the film, calculated using the area density from XRF and the thickness gained from SEM, grown on  $\text{SiO}_2$  is  $\sim 9.2 \text{ g cm}^{-3}$ , which is  $\sim 75\%$  of the bulk value of Ru ( $12.2 \text{ g cm}^{-3}$ ). This relatively low density may constitute one of the reasons for the relatively high resistivity of Ru thin films. A density of  $9.2 \text{ g cm}^{-3}$  is also comparable to other reports.<sup>9</sup>

The resistivity did not show any abrupt variation with increasing  $O_2$  flow rate. It has been reported that  $\text{RuO}_x$  ( $x \sim 2$ ) films are formed when the Ru-source/ $O_2$  ratio decreases to a certain value in Ru ALD using  $\text{Ru}(\text{EtCp})_2$  and  $O_2$ .<sup>8</sup> No increase in the resistivity with increasing  $O_2$  injection time up to 5 s is shown in Fig. 3, and this suggests that  $\text{RuO}_x$  was not formed under these ALD conditions. This can be further confirmed from the AES results shown in Fig. 4.

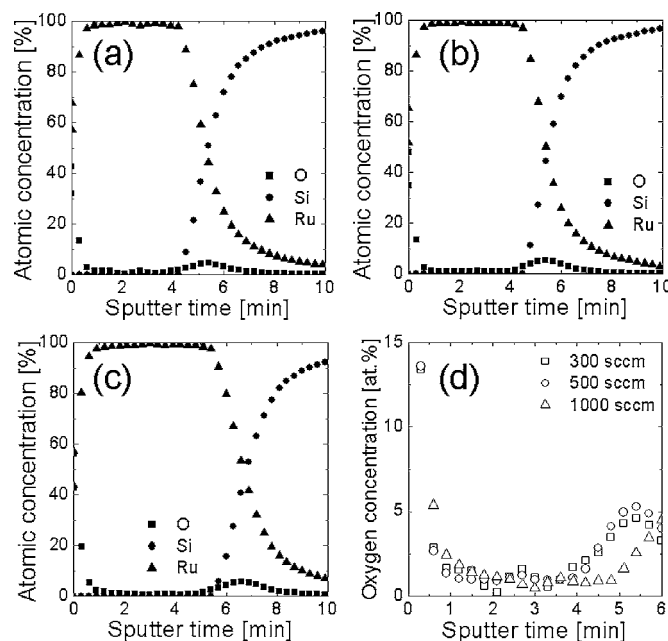
Figure 4a-c shows the AES depth profile results of Ru films grown on Si at a wafer temperature of  $250^\circ\text{C}$  with an  $O_2$  injection time of 2, 3, and 5 s, respectively, and d shows the collected O data from the three samples. The residual oxygen concentration in the Ru layer was negligible up to an  $O_2$  injection time of 3 s. However, it increased to  $\sim 2\text{--}3\%$  when the  $O_2$  injection time increased to 5 s. The relatively high O concentration at the Ru/Si interface was due to the presence of native  $\text{SiO}_2$ .

Figure 5a-c shows the AES depth profile results of the Ru films grown on Si at a wafer temperature of  $280^\circ\text{C}$  with an  $O_2$  flow rate of 300, 500, and 1000 sccm, respectively, and d shows the collected O data from the three samples. Here, the  $O_2$  injection time was 3 s. Different from the deposition results at  $250^\circ\text{C}$ , all the films contained 1–2% of oxygen. This might be due to the slightly increased oxidation rate of the grown Ru film. Therefore, the optimum deposition temperature was  $\sim 250^\circ\text{C}$ .



**Figure 4.** AES depth profile of Ru films grown on Si at a growth temperature of  $250^\circ\text{C}$  with an  $O_2$  injection time of (a) 2, (b) 3, (c) 5 s, and (d) collected oxygen data from the three samples.

Although the direct comparison of the present experiment with other reports where a  $\text{RuO}_x$  phase was observed for a low Ru-source  $[\text{Ru}(\text{EtCp})_2]/O_2$  ratio<sup>8</sup> is difficult due to the different geometries of the reactors and other conditions, it is quite certain that the  $O_2$  flow rate and time in this experiment were excessive (1000 sccm with 2–5 s vs 10–60 sccm with 10–25 s). Considering the similar  $G_r^{\text{sat}}$  of both experiments ( $\sim 0.04 \text{ nm/cycle}$ ), it might be reasonable to compare the oxidation behavior of the deposited Ru films based on the



**Figure 5.** AES depth profile of Ru films grown on Si at a growth temperature of  $280^\circ\text{C}$  with an  $O_2$  flow rate of (a) 300, (b) 500, (c) 1000 sccm, and (d) collected oxygen data from the three samples.



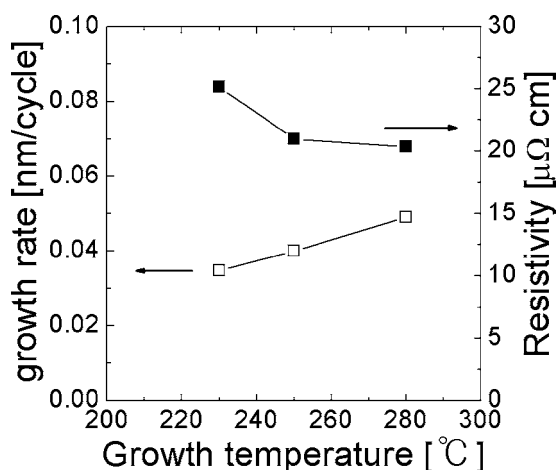
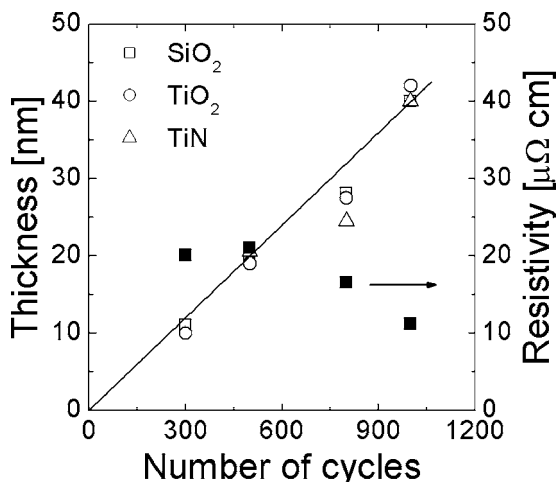


**Figure 6.** The variations in the growth rate and resistivity of a Ru film as a function of the growth temperature.

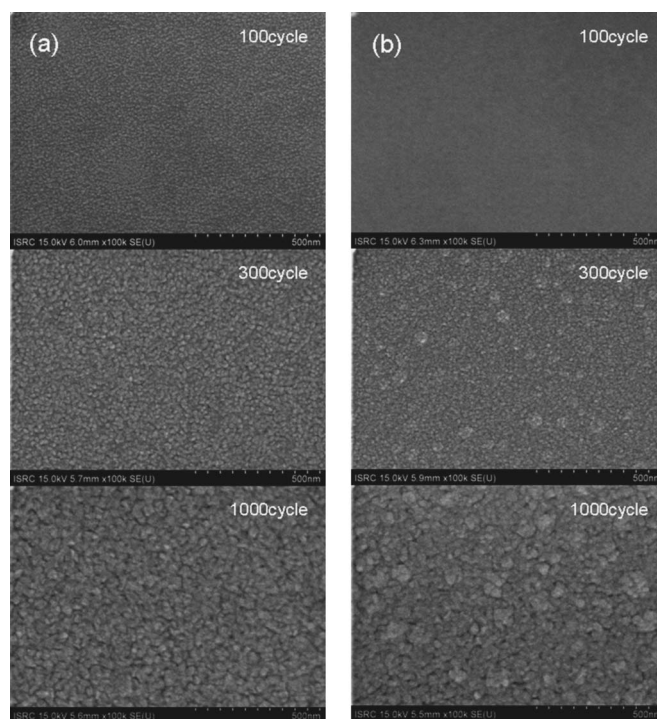
different structures of the Ru precursors [ $\text{Ru}(\text{EtCp})_2$  vs DER]. This is discussed later in conjunction with the negligible incubation period of the present experiment.

Figure 6 shows the variations in  $G_r$  and the resistivity of a Ru film as a function of the growth temperature. Here, the Ru source, Ar carrier, and  $\text{O}_2$  injection times were 6 ms, 3 s, and 3 s, respectively. The growth rate slightly increased with temperature from 0.036 nm/cycle at 230°C to 0.05 nm/cycle at 280°C. The slight increase in  $G_r$  might be due to the increase in the activity of the ALD reaction with increasing temperature. In a report on the MOCVD of Ru using the same precursor and  $\text{O}_2$ , Shibutani et al. showed that  $G_r$  increases with increasing growth temperature from 260 to 300°C by almost 10 times.<sup>16</sup> Although the investigated growth temperature region was slightly different, the relatively small change in  $G_r$  of the present experiment suggests that the ALD window was maintained in this temperature region.

Figure 7 shows the variations in the film thickness (measured by cross-sectional SEM) and resistivity as a function of  $n_{\text{cy}}$  on  $\text{SiO}_2$ ,  $\text{TiO}_2$ , and TiN substrates. Here, the growth temperature, Ru source, Ar carrier, and  $\text{O}_2$  gas injection times were 250°C, 6 ms, 3 s, and 3 s, respectively. The resistivity was measured for a film grown on a  $\text{SiO}_2$  surface. It can be observed that the film thickness increases linearly with increasing  $n_{\text{cy}}$  with an almost identical slope independent of the substrates types. The slope corresponds to a growth rate



**Figure 7.** The variations in the film thickness and resistivity as a function of  $n_{\text{cy}}$  on  $\text{SiO}_2$ ,  $\text{TiO}_2$ , TiN substrates.



**Figure 8.** SEM images of Ru films grown on (a)  $\text{SiO}_2$  and (b)  $\text{TiO}_2$  substrates.

of 0.04 nm/cycle. There is a negligible incubation period at the initial stage of the film growth (almost zero  $x$ -axis intercept of the linear extrapolated graph) on the three substrates. This is a quite different behavior from the Ru film deposition using  $\text{Ru}(\text{thd})_3$ ,  $\text{Ru}(\text{Cp})_2$ , or  $\text{Ru}(\text{EtCp})_2$  either by ALD or MOCVD where rather long incubation periods were observed on Si,  $\text{SiO}_2$ , and  $\text{Al}_2\text{O}_3$ /borosilicate glass substrates.<sup>4,6,9,12</sup> Kang et al. reported that in MOCVD of Ru using  $\text{Ru}(\text{EtCp})_2$  and  $\text{O}_2$  the incubation period of the Ru film growth was rather long on a Si and  $\text{SiO}_2$  surface but it was negligible on a  $\text{TiO}_2$  surface.<sup>18</sup> When the incubation period was long, the nuclei density was low and a rough Ru film was obtained. They ascribed the substrate dependent film growth to the different interface energy.<sup>18</sup>

Figure 8a and b shows the SEM surface morphologies of Ru films grown on  $\text{SiO}_2$  and  $\text{TiO}_2$  substrates, respectively, with varying  $n_{\text{cy}}$ . The surface morphology of a Ru film grown on a TiN substrate was almost identical to that of the film on a  $\text{TiO}_2$  substrate (data not shown). Films as thin as 4 nm (100 cycles) showed uniform and very smooth morphologies, suggesting that the nucleation of Ru on these substrates was quite active. It appeared that the Ru film on  $\text{TiO}_2$  was slightly rougher than that on  $\text{SiO}_2$ . This might be due to the slightly rougher  $\text{TiO}_2$  compared to  $\text{SiO}_2$ , as shown by the cross-sectional TEM in Fig. 9.

Figure 9a and b shows the low-magnification and high-resolution TEM, respectively, of a 20 nm thick Ru ( $n_{\text{cy}} = 500$ ) film grown on an 8 nm thick  $\text{TiO}_2$  film. The  $\text{TiO}_2$  film was amorphous and Ru was polycrystalline, with a columnar grain structure. The average grain diameter appeared to be 10–15 nm. It appeared that there was a negligible interfacial reaction between the Ru and  $\text{TiO}_2$  layers. The Ru film adhesion was quite stable, whereas that on  $\text{SiO}_2$  was worse than that on  $\text{TiO}_2$ .

The present results are also consistent with the report on Ru MOCVD by Shibutani et al., in which they reported the Ru deposition behavior on TiN substrates using DER and  $\text{Ru}(\text{EtCp})_2$  at 275

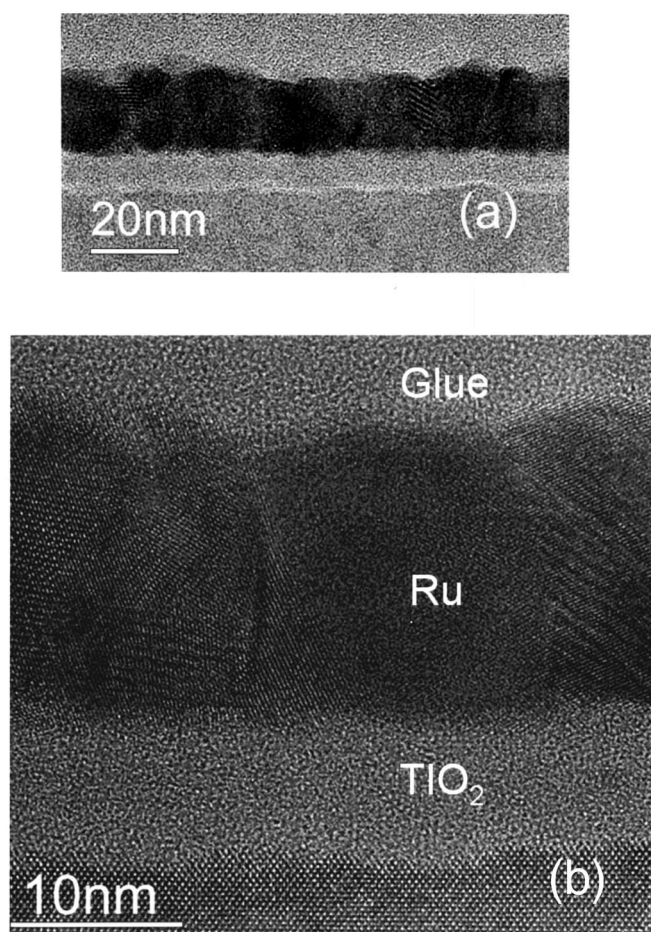


**Figure 9.** (a) Low magnification and (b) high-resolution TEM images of a 20 nm thick Ru film grown on an 8 nm thick  $\text{TiO}_2$  film.

and 350°C. They showed that the DER precursor does not involve any incubation period but the  $\text{Ru}(\text{EtCp})_2$  precursor results in a quite extensive incubation period at both temperatures.

As discussed in detail previously, the ALD of Ru films using  $\text{Ru}(\text{thd})_3$ ,  $\text{Ru}(\text{Cp})_2$ , and  $\text{Ru}(\text{EtCp})_2$ , and  $\text{O}_2$  proceeds with the oxidative dissociation of the ligands. Because the oxidative dissociation also proceeds during the Ru-precursor injection periods,<sup>10</sup> the supply of oxygen to the incoming Ru precursor from the predeposited Ru surface was the key factor. Because the Si,  $\text{SiO}_2$ , and TiN surfaces are generally not favorable surfaces for oxygen donation, the ALD of Ru films suffered from poor nucleation at the initial stage of the film growth.

The negligible incubation period of the present experiment on the three substrate types suggests that the removal of DMPD ligand from the DER molecule does not require such an amount of oxygen supply due to less stable bonding between the DMPD ligand and Ru ions. However, it is expected that the removal of DMPD ligand does not proceed by pure thermal decomposition because proper film growth was not achieved without oxygen. The occurrence of a saturated growth with Ru precursor and  $\text{O}_2$  supply (Fig. 2 and 3) also suggests that the growth is driven by the ALD mechanism and not by a thermal decomposition mechanism. This suggests that the ALD of Ru films using DER requires less oxygen compared to  $\text{Ru}(\text{EtCp})_2$ , although the direct comparison was not made using the same deposition system. This will be the next topic of research.

The use of DER as precursor did not induce  $\text{RuO}_x$  formation and a lower concentration of residual oxygen even at very high oxygen doses (1000 sccm, 5 s injection time). This can be understood from the different oxygen reactivities of DMPD and EtCp ligands. When

the  $\text{Ru}(\text{EtCp})_2$  molecules adsorbed on the predeposited Ru surface which actually contained oxygen, they reacted with the oxygen that was supplied from the predeposited Ru layer. The EtCp ligands become very unstable after dissociation from Ru ions by the disruption of the  $\pi$ -conjugated electron structure. Then, they may instantaneously react with oxygen, resulting in  $\text{CO}_2$  and  $\text{H}_2\text{O}$  formation as shown by the research group at Helsinki University.<sup>10</sup> During the  $\text{O}_2$  supply step a similar reaction may occur between the remaining EtCp ligand on the film surface and the incoming  $\text{O}_2$  leaving the oxygen containing Ru surface again. If the oxygen supply was excessive an oxidation of the Ru film might be possible under these circumstances.

When DER precursor was used instead of  $\text{Ru}(\text{EtCp})_2$ , the reaction may have proceeded in the following way: During the oxygen injection step, oxygen reacts with the EtCp ligand because the DMPD ligand has already been removed in the previous step due to its less stable bonding with Ru ion in DER. As indicated by Aaltonen et al.,<sup>10</sup> the adsorbed oxygen starts to penetrate into the sub-surface after surface saturation has been achieved. The degree of the oxygen penetration is dependent on the surface oxygen concentration. In this experiment, the  $\text{O}_2$  flow rate is excessive (1000 sccm) so that the amount of adsorbed oxygen may be relatively large. Then, DMPD ligand may react with the adsorbed oxygen prior to the EtCp ligand during the subsequent DER injection. The adsorbed oxygen is consumed during this step. This means that the oxygen consumption during the ALD using the DER precursor could be higher than the ALD using the  $\text{Ru}(\text{EtCp})_2$ . It was found that  $\text{RuO}_2$  film growth by MOCVD using DER and  $\text{O}_2$  (up to the  $\text{O}_2$  flow rate of 1000 sccm) at temperatures ranging from 250 to 350°C was not possible from the authors' own experiment. Only Ru films were obtained. However,  $\text{RuO}_2$  films were easily deposited using  $\text{Ru}(\text{EtCp})_2$  and  $\text{O}_2$  with the similar  $\text{O}_2$  flow rate in the same temperature range (data not reported). This also supports that the oxidation of Ru metal atoms derived from DER is relatively difficult in ALD.

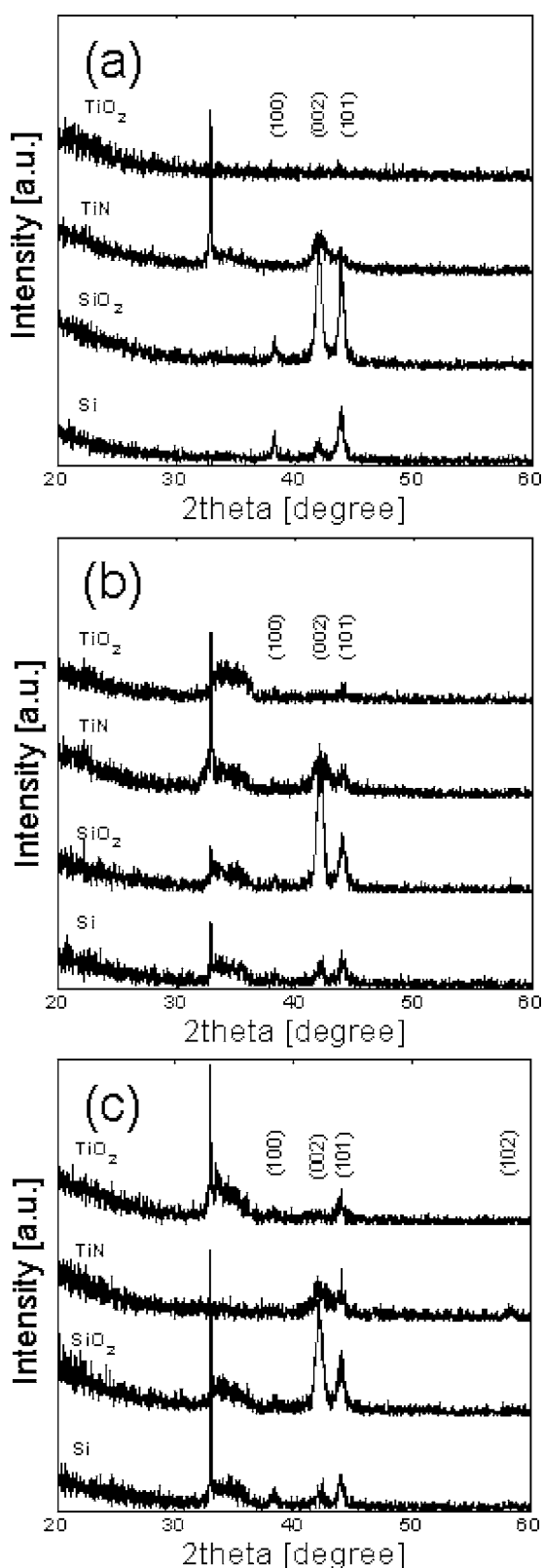
The Ru film growth itself still might be controlled by the removal of the EtCp ligand if the removal of the DMPD ligand is easier than that of the EtCp ligand. This can be confirmed by the similar  $G_r^{\text{sat}}$  (0.04 nm/cycle) of ALD Ru films with either DER or  $\text{Ru}(\text{Cp})_2$ ,<sup>6,10</sup> and comparable activation energies in the ALD window [0.83 eV for DER in this experiment vs 1.06 eV for  $\text{Ru}(\text{Cp})_2$ ].<sup>6,10</sup>

Figure 10a-c shows the XRD patterns of 20 nm thick Ru films grown on Si,  $\text{SiO}_2$ , TiN, and  $\text{TiO}_2$  substrates at 230, 250, and 280°C, respectively. The films grown on Si, TiN, and  $\text{TiO}_2$  substrates show a smaller diffraction peak intensity compared to that on  $\text{SiO}_2$ , suggesting a higher nucleation density and smaller grain size on these substrates, although this was not clearly observed by SEM in Fig. 8. The increase in growth temperature slightly improved the crystalline quality of the Ru films on  $\text{TiO}_2$ , but this could not be observed on Si and TiN. On  $\text{SiO}_2$ , *c*-axis preferential growth became obvious with increasing growth temperature due to the densely packed structure of the (001) plane. This is also consistent with other reports.<sup>4,6,9</sup>

Finally, the step coverage on the capacitor hole structure with an aspect ratio of 17 and a top opening diameter of 150 nm formed in  $\text{SiO}_2$  was investigated. Figure 11a shows the SEM cross section of the hole with the Ru layer grown on top under the following growth conditions; deposition temperature 250°C, Ru source injection time 6 ms, Ar carrier gas flow rate of 30 sccm with an injection time of 3 s,  $\text{O}_2$  flow rate of 1000 sccm with an injection time of 3 s. A Ru film step coverage (defined by bottom thickness/top thickness) of >90% was obtained, which is the best value reported to the best of the authors' knowledge. Figure 11b shows the magnified images of top and bottom portion of the hole.

However, the step coverage was not necessarily guaranteed under other process conditions. For the otherwise given conditions, the Ar carrier gas flow rate had a profound influence on the step cover-





**Figure 10.** XRD patterns of 20 nm thick Ru films grown on Si, SiO<sub>2</sub>, TiN, TiO<sub>2</sub> substrates at the growth temperature of (a) 230, (b) 250, (c) 280°C.

age as shown in Fig. 11c-e. In Fig. 11c-e, the top and bottom portion of the hole with Ar carrier gas flow rates of 100, 300, and 500 sccm, respectively, are shown. Figure 11f shows the variation in the step coverage as a function of the Ar carrier gas flow rate. The step

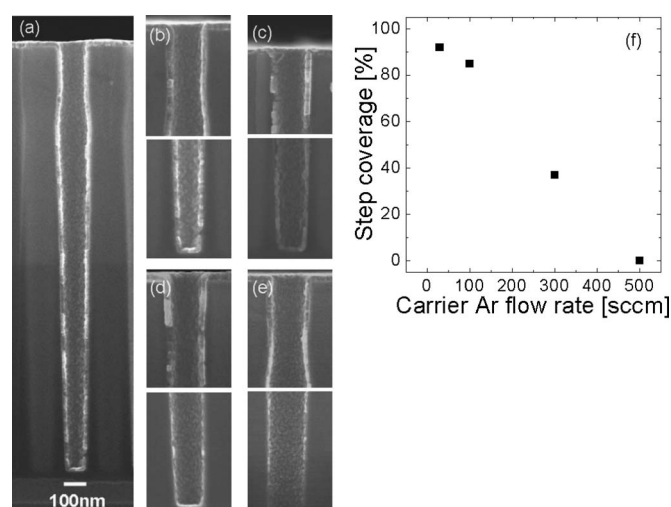


**Figure 11.** (a) Cross-sectional SEM images of the hole structure with the Ru layer. The magnified images of the top and bottom portion of the hole with Ar carrier gas flow rates of (b) 30, (c) 100, (d) 300, (e) 500 sccm, respectively. (f) The variation in the step coverage as a function of the Ar carrier gas flow rate.

coverage severely degraded with an increasing Ar carrier gas flow rate, although the Ru film thickness on the upper part of the hole structure was almost identical. At 500 sccm, almost no Ru film was grown on the bottom area. The negligible change in the film thickness on top and the decreasing film thickness on the bottom with increasing carrier gas flow rate suggests that the degradation in step coverage was not due to the change in the sticking property of the precursor. For the given precursor pulse injection time an increased Ar carrier gas flow resulted in a decrease in the Ru precursor concentration in the gas phase inside the ALD reactor. When the precursor concentration decreased to a low value it could be lower than the minimum gas phase concentration that guaranteed  $G_r^{\text{sat}}$  deep inside the hole. Then,  $G_r$  decreased on the deep hole region which resulted in the poor step coverage.

### Conclusion

Ru thin films were grown on Si, SiO<sub>2</sub>, TiO<sub>2</sub>, and TiN substrates using DER and O<sub>2</sub> as Ru precursor and reactant, respectively, at temperatures ranging from 230 to 280°C by ALD. The best deposition temperature appears to be 250°C considering the saturated growth rate (0.04 nm/cycle) and low oxygen concentration (below the detection limit of AES). DER precursor showed a wider ALD window in terms of the oxygen dose. Active film growth was achieved even from the initial state of the deposition irrespective of the substrate types. Negligible RuO<sub>2</sub> was formed even with an excessive oxygen dose. The film showed a smooth surface, suggesting that nucleation was active by virtue of the DMPD ligand. A high enough step coverage (>90%) was obtained from the Ru film grown on a capacitor hole with an aspect ratio of 17 and an opening diameter of 150 nm by a proper control of the Ar carrier gas flow rate.

### Acknowledgment

The work was supported by the System IC 2010 program and the 0.1 Tbit NVM project of the Korean government. C.S.H. gratefully acknowledges the supply of DER precursor by Tosoh Co.

Seoul National University assisted in meeting the publication costs of this article.

### References

1. H. Kim, *Surf. Coat. Technol.*, **200**, 3104 (2006).
2. M. L. Green, M. E. Gross, L. E. Papa, K. J. Schnoes, and D. Brasen, *J. Electro-*

- chem. Soc.*, **132**, 2677 (1985).
3. Q. Wang, J. G. Ekerdt, D. Gay, Y.-M. Sun, and J. M. White, *Appl. Phys. Lett.*, **84**, 1380 (2004).
  4. T. Aaltonen, M. Ritala, K. Arstila, J. Keinonen, and M. Leskelä, *Chem. Vap. Deposition*, **10**, 215 (2004).
  5. M. Kadoshima, T. Nabatame, M. Hiratani, Y. Nakamura, I. Asano, and T. Suzuki, *Jpn. J. Appl. Phys., Part 2*, **41**, L347 (2002).
  6. T. Aaltonen, P. Alén, M. Ritala, and M. Leskelä, *Chem. Vap. Deposition*, **9**, 45 (2003).
  7. T. Aaltonen, M. Ritala, Y.-L. Tung, Y. Chi, K. Arstila, K. Meinander, and M. Leskelä, *J. Mater. Res.*, **19**, 3353 (2004).
  8. O.-K. Kwon, J.-H. Kim, H.-S. Park, and S.-W. Kang, *J. Electrochem. Soc.*, **151**, G109 (2004).
  9. O.-K. Kwon, S.-H. Kwon, H.-S. Park, and S.-W. Kang, *J. Electrochem. Soc.*, **151**, C753 (2004).
  10. T. Aaltonen, A. Rahtu, M. Ritala, and M. Leskelä, *Electrochem. Solid-State Lett.*, **6**, C130 (2003).
  11. S. Y. Kang, K. H. Choi, S. K. Lee, C. S. Hwang, and H. J. Kim, *J. Electrochem. Soc.*, **147**, 1161 (2000).
  12. H. Han, J. J. Kim, and D. Y. Yoon, *J. Vac. Sci. Technol. A*, **22**, 1120 (2004).
  13. Y. Matsui, M. Hiratani, T. Nabatame, Y. Shimamoto, and S. Kimura, *Electrochem. Solid-State Lett.*, **4**, C9 (2001).
  14. S. Y. Kang, H. J. Lim, C. S. Hwang, and H. J. Kim, *J. Korean Phys. Soc.*, **44**, 25 (2000).
  15. O.-K. Kwon, S.-H. Kwon, H.-S. Park, and S.-W. Kang, *Electrochem. Solid-State Lett.*, **7**, C46 (2004).
  16. T. Shibutami, K. Kawano, N. Oshima, S. Yokoyama, and H. Funakubo, *Electrochem. Solid-State Lett.*, **6**, C117 (2003).
  17. S. Y. Kang, H. J. Lim, C. S. Hwang, and H. J. Kim, *J. Electrochem. Soc.*, **149**, C317 (2002).
  18. S. Y. Kang, C. S. Hwang, and H. J. Kim, *J. Electrochem. Soc.*, **152**, C15 (2005).